

Accepted Manuscript

Comparative study of graphene nanoparticle and multiwall carbon nanotube filled epoxy nanocomposites based on mechanical, thermal and dielectric properties

Muhammad Razlan Zakaria, Muhammad Helmi Abdul Kudus, Hazizan Md Akil, Mohd Zharif Mohd Thirmizir



PII: S1359-8368(16)31792-9

DOI: [10.1016/j.compositesb.2017.03.023](https://doi.org/10.1016/j.compositesb.2017.03.023)

Reference: JCOMB 4957

To appear in: *Composites Part B*

Received Date: 30 August 2016

Revised Date: 14 March 2017

Accepted Date: 15 March 2017

Please cite this article as: Zakaria MR, Kudus MHA, Akil HM, Thirmizir MZM, Comparative study of graphene nanoparticle and multiwall carbon nanotube filled epoxy nanocomposites based on mechanical, thermal and dielectric properties, *Composites Part B* (2017), doi: 10.1016/j.compositesb.2017.03.023.

This is a PDF file of an unedited manuscript that has been accepted for publication. As a service to our customers we are providing this early version of the manuscript. The manuscript will undergo copyediting, typesetting, and review of the resulting proof before it is published in its final form. Please note that during the production process errors may be discovered which could affect the content, and all legal disclaimers that apply to the journal pertain.

Comparative study of graphene nanoparticle and multiwall carbon nanotube filled epoxy nanocomposites based on mechanical, thermal and dielectric properties

Muhammad Razlan Zakaria^a, Muhammad Helmi Abdul Kudus^a, Hazizan Md. Akil^{a,b*},
Mohd Zharif Mohd Thirmizir^b

^aSchool of Materials and Mineral Resources Engineering, Engineering Campus,
Universiti Sains Malaysia, 14300 Nibong Tebal, Pulau Pinang, Malaysia.

^bCluster for Polymer Composite (CPC), Science and Engineering Research Center,
Engineering Campus, Universiti Sains Malaysia, 14300 Nibong Tebal, Pulau Pinang,
Malaysia.

*Corresponding email: hazizan@usm.my
Tel:04-5996161, Fax: 04-5941011

Abstract

Nano-sized carbons, such as graphene nanoparticle (GNP) and multiwall carbon nanotube (MWCNT), have attracted a great deal of attention due to their extraordinary intrinsic properties. Extensive research has been done on each carbon material for epoxy nanocomposites but only a few have ventured into a comparison study. In this paper, the effect of GNP and MWCNT, at various filler loadings, on the mechanical, thermal and dielectric properties of epoxy nanocomposites have been investigated. The experimental results demonstrate that GNP filled epoxy nanocomposites showed higher thermal and dielectric properties, but slightly lower mechanical properties compared to the MWCNT filled epoxy nanocomposites. The tensile strength, flexural strength, thermal conductivity and dielectric constant of GNP filled epoxy nanocomposites improved up to 11%, 17%, 126%, and 171% respectively, and MWCNT filled epoxy nanocomposites improved up to 26%, 29%, 60%, and 73% respectively.

Keywords: Graphene; Carbon nanotubes; Polymer-matrix composites (PMCs);

Epoxy nanocomposites

1.0 Introduction

Epoxy resin belongs to a major class of engineering polymeric materials and is extensively used as a matrix for polymer composites due to its excellent chemical and heat resistances, low shrinkage upon curing and relatively high strength and modulus [1] [2] [3] and [4]. During the last few decades, epoxy nanocomposites with carbon-based nanofillers have been extensively investigated in fabricating materials with multifunctional properties, such as high mechanical, thermal and electrical performances. Furthermore, within the last few years, large number of researches have been conducted in performing multifunctional epoxy nanocomposites based on carbon nanotubes (CNTs) and graphene, due to the extraordinary intrinsic properties of these fillers [5] [6] [7] [8] [9] and [10].

CNTs were discovered by Iijima in 1991 [11], followed by graphene - also known as the mother of all graphitic materials - in 2004 [12]. Since the advent of CNTs and graphene, the scientific community's interest on these two nanomaterials has grown exponentially; and the number of publications written on these materials has increased dramatically [13] [14] [15] and [16]. CNTs are one-dimensional with a cylindrical nanostructure, while graphene is two-dimensional with a sheet nanostructure. These two nanomaterials are both sp^2 hybridized carbon atoms that are densely packed in a honeycomb crystal lattice; but distinctly different in geometry. CNTs and graphene were reported to possess superior mechanical properties, with Young's modulus of 0.27 - 0.95 TPa [17] and 1 TPa [18] respectively, and ultimate strengths of 11 - 63 GPa [17] and 130 GPa, [18] respectively. CNTs and graphene are also predicted to give remarkable performances in areas such as thermal and electrical conductivity. Thermal and electrical conductivity for CNTs is up to 3,000 W/mK [19] and 1800 S/cm, [20] respectively. Meanwhile, the thermal and electrical conductivity

for graphene is up to 5,000W/mK [21] and 6,000S/cm, [22] respectively. Due to their remarkable mechanical, thermal and electrical properties, it is believed that small amounts of CNTs and graphene can significantly improve the performance of epoxy nanocomposites [23] [24] [25] [26]. Despite the mechanical properties of CNTs being on a par with graphene, the latter remains a better material than CNTs in certain aspects, such as thermal and electrical conductivity. Furthermore, recent studies have also shown that graphene surpasses the properties of CNTs [27]. This is attributed to the incredibly high specific surface area, unique graphitised plane structure and the extremely high charge mobility of graphene [28] and [29].

The purpose of this study was to compare the effects of CNTs and graphene on the mechanical, thermal and dielectric properties of epoxy nanocomposites. Even though some comparisons have been reported previously regarding CNTs and graphene, the effect of these two fillers within the range of 0.5 – 3 wt% on mechanical, thermal and dielectric properties are yet to be reported. Therefore, our characterization and assessment provides additional information pertaining to the comparison between CNTs and graphene. This study has also identified new and significant information that would be of interest to researchers and industrialists working on epoxy nanocomposites, in order for them to make a good selection between these two fillers for various applications.

In this study, the morphology and characteristics of the CNTs and graphene were observed using Field Emission Scanning Electron Microscope (FESEM) and High Resolution Transmission Electron Microscope (HRTEM). Tensile and flexural tests were done on the CNTs and graphene filled epoxy nanocomposites. The FESEM and HRTEM observation were performed on the fracture surface of the CNTs and graphene filled epoxy nanocomposites to evaluate the dispersion of fillers and the

fracture mechanism. Thermal conductivity was measured using a Hot Disk Thermal Constants Analyser and the dielectric constant was identified using RF Impedance. The possible explanations for comparisons between the CNTs filled epoxy nanocomposites and graphene filled epoxy nanocomposites are discussed below.

2.0 Experimental

2.1 Materials

Industrial grade graphene nanopowder (GNP) and multi-walled carbon nanotubes (MWCNT) were purchased from SkySpring Nanomaterials Inc. The GNP constituted of a few sheets of graphene stacked together and had a particle diameter of about 15 μ m. The sheet thickness of GNP ranged from 11 to 15 nm. The MWCNT had an outside diameter of 10-20 nm and inside diameter of 3-5nm with a length in a range of 5-30 μ m. The purity of the GNP and MWCNT were 95% and 99.5% respectively. The epoxy resin and curing agent were used in polymer nanocomposites are DER 331 and Epoxy Hardener Clear. The DER 331 and Epoxy Hardener Clear were purchased from Eurochemo Pharma Sdn. Bhd.

2.2 Preparation of CNT and GNP epoxy nanocomposites

The GNP and MWCNT were first dispersed in DER 331 at the frequency of 25kHz using a QSonica sonicator machine for 30 minutes. The temperature of the mixture was maintained in the range of 60°C-70°C to avoid damage to the structure of MWCNT and GNP structure. Then, the curing agent (Epoxy Hardener Clear) was poured into the mixture at a mass ratio of 6:10 to the epoxy resin. After that, the mixture was placed in a vacuum in order to remove air bubbles at 76cm Hg pressure

for 30 minutes. Finally, the epoxy nanocomposites were poured into a silicon mould and cured at 120°C for 1 hour. The epoxy nanocomposites were prepared with various filler loadings of GNP and MWCNT contents. Table 1 depicted the descriptions of the composite samples.

2.3 Characterization of CNT and GNP

The X-ray diffraction system (Model: Philips X-Pert Pro Diffractometer) was used to characterize the GNP and MWCNT crystallographic structures in the 2θ range of 10–80°. The morphologies of the GNP and MWCNT were analysed by using a field emission scanning electron microscope (FESEM) (Model: LEO SUPRA 35VP, Carl Zeiss, Germany) and a high resolution transmission electron microscope (HRTEM) (Model: Philip TECNAI 20). The structural characteristics of the GNP and MWCNT were analysed using Raman spectroscopy (Renishaw inVia Raman spectrometer).

2.4 Characterization of epoxy nanocomposites

Universal testing machine (Model: 5982, Instron, USA) were used to perform tensile and flexural tests of the Epoxy/GNP and Epoxy/MWCNT. The tensile and flexural specimens were prepared and tested according to ASTM D638 standard and ASTM D790 standard respectively. Five specimens for each samples were tested to ensure the reliability of the test results. The fracture surfaces from tensile tested specimens were analysed by FESEM after being coated with a 5–10nm Au-Pd layer through sputtering. The morphology of Epoxy/GNP and Epoxy/MWCNT at nano-scale were analysed using HRTEM. Cryo-ultramicrotomy was perform using Leica (Model: Reichert-Jung Ultracut E) to prepare the samples with 50nm thickness. Hot Disk Thermal Constants Analyser (Model: TPS 2500 S) was used to determine thermal conductivity of the Epoxy/GNP and Epoxy/MWCNT with specimen size of 30mm in

diameter and 10mm in thickness. RF Impedance (Model: Hewlett Packard 4219B) was performed at frequency range of 500MHz to 1GHz to measure dielectric constant of the Epoxy/GNP and Epoxy/MWCNT. Dimension of the samples was 30mm in diameter and 2mm in thickness.

3.0 Results and Discussion

3.1 Analysis of GNP and MWCNT

The surface morphologies of the GNP and MWCNT were characterized by SEM. Fig. 1a shows the SEM images of the GNP with a typical crumpled structure. This typical thin sheet structure makes the GNP have a huge specific surface area. From the SEM observation, the diameter of the GNP is about 10 - 20 μ m and its thickness ranged from 11 - 15nm, which consisted of a few sheets of graphene stacked together. In addition, it was observed that some GNP nanosheets superimposed on top of each other and wrinkled into an irregular shape. Fig. 1b displays the morphological structure of MWCNT. It is clear that the MWCNT were tubular in structure and uniformed in distribution. The diameter of the MWCNT was about 10 -20nm.

Fig. 2 shows HRTEM images of the GNP and MWCNT. The HRTEM image of the GNP in Fig. 2a shows that the GNP nanosheet looks like wrinkled or crumpled thin paper. The high magnification image of the edge of the GNP nanosheet is shown in Fig. 2b. From the figure, it can be observed that the planer few layer graphene structures consists of 26 numbers of graphitic layers. The HRTEM image in Fig. 2c shows the MWCNT, which are randomly organized and aggregated owing to inter-molecular Van der Waals' interaction which form entanglements in certain areas. From closer observations of the MWCNT structure, as shown in Fig. 2d, the

MWCNT had 15–25 walls of graphitized carbon and an inner hollow diameter of 4–8nm. The diameter of the tube was 15nm, which coincided approximately with the diameter estimated from the SEM image. For the crystal face spacing distance between walls, both GNP and MWCNT show the value of $\sim 0.34\text{nm}$ which indicate the ideal structure for graphite in GNP and MWCNT. Li and Chou have discussed a theoretical concept of crystal face spacing between the structural and molecular in graphite [30]. The carbon atoms in graphite are arranged at the corners of hexagons and covalently bonded to each other with $\sim 0.14\text{nm}$ carbon–carbon distance. Meanwhile, the interlayer distance of the graphite layer was $\sim 0.34\text{nm}$ which was weakly bounded through Van der Waals' interaction.

A diffraction pattern is created when X-rays interact with a crystalline substance (phase). The XRD pattern of a pure substance can be described as an identification of the substance because the same substance always gives the same pattern. The main features of the XRD pattern of GNP and MWCNT are close to those of graphite due to their intrinsic nature. Fig. 3 shows the XRD patterns of GNP (curve a) and MWCNT (curve b). The diffractograms of GNP and MWCNT displayed the existence of carbon (C). Both the GNP and MWCNT exhibited a (0 0 2) peak at $2\theta=26^\circ$ due to the presence of C, which indicated the presence of well-crystallized graphite. As seen in Fig. 3, the intensity of the GNP peak is higher and sharp compared to MWCNT. This is due to the fact that X-ray diffraction does not measure (0 0 2) peak with well-aligned, straight MWCNT on the substrate surface [31]. In the case of MWCNT, the X-ray incident beam is scattered inside the sample and is not collected when the tube axis perpendicular to the substrate surface. Thus, the intensity of the (0 0 2) peak of MWCNT decreases.

The Raman spectroscopy is a simple yet elegant way to study the structural characteristics of GNP and MWCNT. It was a useful tool in examining the nanocrystalline, crystalline, and amorphous of graphitic base materials [32]. Fig. 4 displays the representative Raman spectra of the GNP and MWCNT samples. The main features of GNP and MWCNT in the Raman spectrum were the irregular induced D-band which represented the characteristics for defects in graphitic structure and disordered carbon ($\sim 1350\text{ cm}^{-1}$); the G-band which indicated the crystalline graphitic and tangent vibrations of sp^2 carbon ($1500\text{--}1600\text{ cm}^{-1}$); and the D*-band which represented the overtone of the disorder ($\sim 2600\text{ cm}^{-1}$) [33]. The GNP Raman spectra showed peaks at 1328 cm^{-1} (D-band), 1580 cm^{-1} (G-band) and 2689 cm^{-1} (D*-band) and MWCNT Raman spectra showed peaks at 1330 cm^{-1} (D-band), 1594 cm^{-1} (G-band) and 2650 cm^{-1} (D*-band). Generally, defects in graphitic structure and the disorders of graphitic base materials are due to finite or nano sized graphitic planes and other forms of carbon, such as vacancies, heptagon–pentagon pairs, rings around the defects on graphitic structure, heteroatoms and kinks [34]. A common method to measure the quality of GNP and MWCNT samples is by analysing the ratio of the intensity of the D-band to the G-band (I_D/I_G) [35]. Usually, materials which have low I_D/I_G ratio are carbon atoms sp^2 bonded with a few defects or high purity. Large quantities of impurities or defects in the sample were indicated by a high I_D/I_G ratio. Based on Table 3, the intensity ratios of the D-band to the G-band (I_D/I_G) of the GNP and MWCNT were calculated as 0.36 and 1.69 respectively. The degree of disorder on the GNP and MWCNT can also be determined by the intensity ratio of the D*-band to the G-band (I_{D^*}/I_G). Higher degree of disorder or a higher defect concentration can be described by increased the value of I_D/I_G or decreased the value of I_{D^*}/I_G . From the result, the MWCNT showed higher value

of I_D/I_G and lower value of I_{D^*}/I_G compared to the GNP. This was attributed to sp^3 bonding defects, and kinks and twists in the structure of the MWCNT. The results reveal that the GNP has the best structure quality. This statement was supported by the previous XRD analysis which showed a sharp peak of carbon in the GNP. Consequently, the high crystalline structures of GNP could have higher thermal conductivity and electrical properties.

3.2 Mechanical properties

Tensile and flexural testing were carried out to investigate the reinforcement effect of GNP and MWCNT on epoxy nanocomposites. Fig. 5 shows the tensile stress–strain curve of Epoxy/GNP and Epoxy/MWCNT at various different filler loadings. Meanwhile, Fig. 6 shows the flexural stress–strain curve of the Epoxy/GNP and the Epoxy/MWCNT at various different filler loadings. Generally, both Epoxy/GNP and Epoxy/MWCNT show an enhancement of the tensile and flexural properties compared to the neat epoxy. This is due to the extraordinary mechanical properties of GNP and MWCNT as fillers. The difference between the Epoxy/GNP and Epoxy/MWCNT are shown in Table 3. It can be seen that the Epoxy/MWCNT showed a higher tensile strength, tensile modulus, flexural strength and flexural modulus compared to the Epoxy/GNP. From the table, it is evident that the highest tensile strength was achieved by the Epoxy/MWCNT1 with an increment of up to about 58.65MPa, which correspond to a 26% increment compared to the neat epoxy. Meanwhile, the Epoxy/GNP 1 also recorded an increment of 11% (51.65MPa) in tensile strength as compared to the neat epoxy. The highest flexural strength of the Epoxy/MWCNT 1 was 126.70MPa, which presented an enhancement of up to 29% compared to the neat epoxy. The highest flexural strength of Epoxy/GNP was achieved at 1wt% with 114.89MPa, and exhibited an enhancement of up to 17%

compared to the neat epoxy. The tensile strength and flexural strength for epoxy composites depends on various factors; including the interfacial adhesion, strength of the matrix material, and the shape and dispersion of particles in the matrix [36]. The dispersion and shape of the GNP and MWCNT in the polymer matrix is one of the most crucial factors to be considered. The higher tensile strength and flexural strength of the Epoxy/MWCNT has been attributed to the fact that two-dimensional GNP is more easily aggregated than MWCNT due to its larger surface areas and plane-to-plane contact areas. Thus, the Van der Waals' force between adjacent GNP may be stronger than those between MWCNT; making the MWCNT easier to disperse than the GNP in the epoxy matrix. In addition, some kinks and twists in the structure of the MWCNT might have prevented the detachment of MWCNT from the epoxy matrix. In comparison, the two-dimensional structure of the GNP, like wrinkled thin film, seemed much easier to detach from the epoxy matrix compared to the MWCNT structure. These factors contribute to the reinforcement efficacy involved in the good interfacial interaction among the fillers and the epoxy matrix. As a result, the load can effectively be transferred from the epoxy matrix to the fillers and therefore the tensile strength and flexural strength could be improved.

The variation of the tensile modulus and flexural modulus of the Epoxy/GNP and Epoxy/MWCNT showed a similar trend as tensile strength and flexural strength. Epoxy/MWCNT 1 shows that the highest tensile modulus was achieved by a 26% increment compared to the neat epoxy which was 1.87GPa. The tensile modulus of the Epoxy/GNP 1 seemed to be the highest among all Epoxy/GNP composites with 1.65GPa, and showed a 11% increment compared to the neat epoxy. The flexural modulus of the Epoxy/MWCNT specimens filled with 1wt% of MWCNT presented the highest flexural modulus with an enhancement of up to 38% compared to the neat

epoxy. Similarly, for Epoxy/GNP, the flexural modulus specimens filled with 1wt% of GNP presented the highest flexural modulus with an enhancement of up to 28% compared to the neat epoxy. The enhancement of tensile modulus and flexural modulus could be related to the addition of the GNP and MWCNT, which restricted the mobility of polymer chains under the load [37]. It is possible that the effect of the addition of the GNP and MWCNT may have increased the cross-link ratio and blocked the molecular motions of the epoxy matrix [38]. Furthermore, the high aspect ratio, high modulus and strength of the GNP and MWCNT also contributed to the enhancement of the tensile modulus and flexural modulus. However, further increment of filler loadings of the GNP and MWCNT, above 3wt%, showed a trend of tensile and flexural properties slightly decreasing. This phenomenon was expected and largely attributed to the agglomeration of the GNP and MWCNT, and the difficulties in dispersing the filler at higher concentrations; especially with the large surface area of the GNP and MWCNT. The GNP and MWCNT tended to stack together owing to their Van der Waals' force, which then formed agglomerations. Thereby, the tensile and flexural properties of the system were reduced because the agglomeration avoids the effective stress distribution and introduces stress concentration, which weakens the matrix. The fracture strain of the epoxy composites reduced with the increasing filler loadings for both the GNP and MWCNT due to the increase in rigidity provided by the rigid fillers. The addition of the GNP and MWCNT caused the epoxy composites to become more brittle and resulted in a decrease in the elongation at break.

In order to understand the enhancement of the tensile and flexural properties of the epoxy nanocomposites, the fracture processes that were taking place on or in the immediate vicinity of the fracture surface were examined by FESEM. Fig. 7a–c

shows the fracture surface of the Epoxy/GNP, which demonstrates the flaky-shape of the GNP at the surface of the epoxy matrix. From the figure, it can be seen that some GNP caused wrinkling and crimping. This is due to the very thin paper-like structure of the GNP, which makes it very flexible and easily deformed. Fig. 8a–c shows the fracture surface of the Epoxy/MWCNT. From the figure, it can be seen that there are small bright dots in the fracture surface, indicating the ends of broken MWCNT. The MWCNT were broken instead of being pulled out of the epoxy matrix, demonstrating that the MWCNT possess a strong interfacial bonding with the epoxy matrix, whereby it can tightly hold the MWCNT through interfacial bonding. This condition resulted in an effective load transfer from matrix to filler, thereby improving the tensile and flexural properties.

The HRTEM was conducted to further study the morphology of the Epoxy/GNP and Epoxy/MWCNT, with a more close-up view at nano scale. Based on the morphology of the Epoxy/GNP, shown in Fig. 9a–b, the GNP seemed to be wrinkled in the epoxy matrix, which was similar to the previous SEM observation. Meanwhile, the morphology of the Epoxy/MWCNT, shown in Fig. 9c–d, illustrated that the MWCNT had distributed randomly within the epoxy matrix.

3.3 Thermal conductivity

As a type of polymer, the pure epoxy resin has poor thermal conductivity. Based on the theories of thermal conduction [39] however, the thermal conductivity of the epoxy resin can be improved by filling it with higher thermal conductivity fillers. The extraordinary thermal properties of MWCNT and GNP are expected to give an epoxy matrix higher thermal conductivity. It is well known that, the heat is transferred

mainly in the form of acoustic phonons in polymer composites. Thus, factors such as fraction, aspect ratio, surface roughness, degree of dispersion, orientation, the intrinsic crystallinity of the filler and the filler-matrix interface thermal contact resistance can affect the overall thermal conductivity of polymer composites [40].

Fig. 10 shows the graph of the thermal conductivity of the neat epoxy, the Epoxy/GNP and the Epoxy/MWCNT with different filler loadings. Based on the graph, it is evident that the Epoxy/GNP and the Epoxy/MWCNT showed a higher thermal conductivity compared to the neat epoxy. The incremental trends of thermal conductivity via the adding of MWCNT and GNP in epoxy nanocomposites has been reported by other researchers on previous occasions [34] [41]. As such, the thermal conducting path or network was the significant factor which contributed to the thermal conductivity improvement of the epoxy nanocomposites. The addition of the MWCNT and GNP into the epoxy matrix acted as a thermal bridge, which efficiently enhanced the heat flow. As a result, the formed thermal chains among the fillers enhanced the thermal conductivity of the epoxy nanocomposites. In addition, the increment in thermal conductivity of the Epoxy/MWCNT and the Epoxy/GNP was also a result of the great level of thermal conductivity of the MWCNT and GNP; both which possessed thermal conductivity up to 3,000W/mK and 5,000W/mK respectively [19] and [21].

The thermal conductivity of the Epoxy/MWCNT and Epoxy/GNP simultaneously increased while increasing the filler loading of MWCNT and GNP. This is because the decrease in distance between fillers could form more thermal chains between the fillers; creating a thermal conducting path or network. At 0.5wt % of filler loading, the thermal conductivity of the epoxy nanocomposites containing MWCNT and GNP increased from 0.21W/mK to 0.24W/mK and 0.27W/mK respectively. As the

MWCNT and GNP concentration was further increased to 3wt %, the Epoxy/GNP still performed at better thermal conductivity compared to the Epoxy/MWCNT.

The Epoxy/GNP 3 showed a thermal conductivity of 0.47W/mK with increment about 126.4% compared to the neat epoxy. Meanwhile, Epoxy/MWCNT 3 showed a thermal conductivity of 0.33W/mK an increase of 60.2% compared to the neat epoxy. This is because the GNP provides better thermal conductivity compared to the CNT due to the two-dimensional sheet structure. In GNP, the phonon can travel in two directions - parallel and perpendicular to the surface. Meanwhile in CNT, the phonon only travels in one direction – along the nanotube, due to its one-dimensional cylindrical structure. Moreover, the phonon moving along the nanotube would be obstructed when the phonon meets the kinks or twists of the CNT [42]. The kinks and twists formed at the CNT would lead to reduce in effective aspect ratio of the CNT. Therefore, decreasing the thermal conductivity of the epoxy nanocomposite.

3.4 Dielectric Constant

The frequency dependence of dielectric constants of the Epoxy/GNP and Epoxy/MWCNT including various weight fractions of the filler were measured over the frequency range of 500MHz to 1GHz at room temperature, and the results are shown in Fig.11. The dielectric constant is of special interest to researchers and engineers as these properties provide insight into GNP and MWCNT suitability for electronic applications. As we know, the dielectric constant of material represents the polarization response of material to an electric field. The effects of the GNP and MWCNT on the dielectric constant of the epoxy nanocomposite depended on their reaction to the polarization process. For heterogeneous polymers, there are a few

factors affecting the dielectric constant such as electronic and atomic orientation and interfacial polarization [43]. In addition, the conductivity of the fillers and the interface adhesion between the fillers and epoxy matrix determined the electric response of the epoxy nanocomposites. Based on the graph, it can be seen that the Epoxy/GNP and the Epoxy/MWCNT showed a higher dielectric constant compared to the neat epoxy. This is due to the addition of the GNP and MWCNT to the epoxy matrix which induced the variation of the polarization process. It was reported that, the GNP and MWCNT, which consist of sp^2 hybridized carbon atoms, exhibit superior electrical properties. The delocalization of the π electrons in hybridized sp^2 makes the electrons free to move when an electric field is applied. As a result, higher conductivity fillers such as GNP and MWCNT lead to the formation of a micro-capacitor and increase the dielectric constant of the epoxy nanocomposites. The formation of the micro-capacitor caused the GNP and MWCNT charges to accumulate when the electric field was applied. Furthermore, the polarizability of the epoxy nanocomposites increased with the increasing of the filler loading because the isolation distance between the fillers reduced simultaneously. This caused more charges to accumulate on the GNP and MWCNT and thus increased the dielectric constant of the epoxy nanocomposites.

In comparison, the Epoxy/GNP showed a higher dielectric constant compared to the Epoxy/MWCNT. The dielectric constant slightly increased at 0.5wt% of filler loading. However, at above 1wt% of filler loading, a significant increment in the dielectric constant was observed. The highest dielectric constant was achieved by the Epoxy/GNP 3, with an increment of up to 9.05, which corresponded to a 171% increment compared with the neat epoxy at 1GHz. The high dielectric constant of the Epoxy/GNP may be attributed to the ability of the GNP to produce large amounts of

micro-capacitors compared to the MWCNT. This is due to the good quality of structure of the GNP compared to MWCNT, based on the Raman spectroscopy analysis. Furthermore, the GNP was also reported to possess better electrical properties than the MWCNT [27]. As shown in the figure, the dielectric constant for all investigated composite systems decreased with the increase in frequency. The decrease of the dielectric constant when compared with the frequency was associated to the decrease of total polarization arising from dipoles. In dielectric materials, the electric dipoles tend to align with the applied field. At low frequency, the low rate of alteration of the electric field makes dipoles orient themselves easily in the direction of the alternating field, which leads to a high dielectric constant. At a higher frequency, the inability of dipoles to easily change the direction of orientation with the increasing rate of the alteration of the applied field leads to a lower dielectric constant.

In electronic application, low value of dielectric loss is favorable due to the low energy loss. In this study, the effect of GNP and MWCNT addition as well as the amount of each fillers is evaluated and compared as shown in Fig. 12. From the figure, it can be seen that the dielectric loss of the Epoxy/GNP and the Epoxy/MWCNT increased with increasing filler loading in the epoxy matrix. This is because when the filler loading of GNP and MWCNT increased, highly conductive of GNP and MWCNT particle easily formed a conductive path in the Epoxy/GNP and Epoxy/MWCNT. Thus, leakage current will occur when Epoxy/GNP and Epoxy/MWCNT become more conductive as filler increases and cause part of the electrical energy to be transformed into thermal energy [44]. For comparison, it can be seen that the Epoxy/GNP showed a higher dielectric loss compared to the Epoxy/MWCNT for a given filler loading of 0.5wt%, 1wt% and 3wt%. This is

because, Epoxy/GNP is more conductive than Epoxy/MWCNT due to the GNP possess better electrical properties than the MWCNT as discussed previously.

4.0 Conclusion

This study investigated the effect of GNP and MWCNT on the mechanical, thermal and dielectric properties of epoxy nanocomposites at various filler loadings. Based on the experimental findings, it can be concluded that the incorporation of GNP and MWCNT in epoxy creates a significant impact on the properties of the epoxy nanocomposites. The Epoxy/GNP showed higher thermal and dielectric properties but slightly lower mechanical properties compared to the Epoxy/MWCNT. The tensile strength and flexural strength of the Epoxy/GNP were enhanced about 11% and 17% respectively, whereas the tensile strength and flexural strength of the Epoxy/MWCNT were enhanced to about 26% and 29% respectively. The thermal conductivity and dielectric constant of the Epoxy/GNP showed significant improvement of up to 126% and 171% respectively, and the Epoxy/MWCNT showed an improvement up to 60% and 73% respectively. MWCNT possess strong interfacial interactions between fillers and the matrix compared to GNP, which leads to higher mechanical properties. However, based on the XRD and Raman analysis, GNP possesses better structure quality compared to MWCNT, which results in higher thermal and dielectric properties.

Acknowledgement

The authors would like to acknowledge Universiti Sains Malaysia (USM) FRGS 203/PBAHAN/6071337 for sponsoring and providing financial assistance during this research work.

References

- [1] Kumar A, Ghosh PK, Yadav KL, Kumar K. Thermo-mechanical and anti-corrosive properties of MWCNT/epoxy nanocomposite fabricated by innovative dispersion technique. *Compos Part B-Eng.* 2017;113:291-9.
- [2] Liu W, Wang Y, Wang P, Li Y, Jiang Q, Hu X, et al. A biomimetic approach to improve the dispersibility, interfacial interactions and toughening effects of carbon nanofibers in epoxy composites. *Compos Part B-Eng.* 2017;113:197-205.
- [3] Shiu S-C, Tsai J-L. Characterizing thermal and mechanical properties of graphene/epoxy nanocomposites. *Compos Part B-Eng.* 2014;56:691-7.
- [4] Pascault J-P, Williams RJ. *Epoxy polymers*: John Wiley & Sons; 2009.
- [5] Tang L-C, Wan Y-J, Yan D, Pei Y-B, Zhao L, Li Y-B, et al. The effect of graphene dispersion on the mechanical properties of graphene/epoxy composites. *Carbon.* 2013;60:16-27.
- [6] Rafiee MA, Rafiee J, Wang Z, Song H, Yu Z-Z, Koratkar N. Enhanced Mechanical Properties of Nanocomposites at Low Graphene Content. *ACS Nano.* 2009;3(12):3884-90.
- [7] Moriche R, Prolongo SG, Sánchez M, Jiménez-Suárez A, Sayagués MJ, Ureña A. Morphological changes on graphene nanoplatelets induced during dispersion into an epoxy resin by different methods. *Compos Part B-Eng.* 2015;72:199-205.
- [8] Gojny FH, Wichmann MHG, Köpke U, Fiedler B, Schulte K. Carbon nanotube-reinforced epoxy-composites: enhanced stiffness and fracture toughness at low nanotube content. *Compos Sci Technol.* 2004;64(15):2363-71.
- [9] Kim MT, Rhee KY, Jung I, Park SJ, Hui D. Influence of seawater absorption on the vibration damping characteristics and fracture behaviors of basalt/CNT/epoxy multiscale composites. *Compos Part B-Eng.* 2014;63:61-6.
- [10] Montazeri A, Javadpour J, Khavandi A, Tcharkhtchi A, Mohajeri A. Mechanical properties of multi-walled carbon nanotube/epoxy composites. *Mater Design.* 2010;31(9):4202-8.
- [11] Iijima S. Helical microtubules of graphitic carbon. *Nature.* 1991;354(6348):56-8.
- [12] Novoselov KS, Geim AK, Morozov S, Jiang D, Zhang Y, Dubonos Sa, et al. Electric field effect in atomically thin carbon films. *Science.* 2004;306(5696):666-9.
- [13] Tan QC, Shanks RA, Hui D, Kong I. Functionalised graphene-multiwalled carbon nanotube hybrid poly(styrene-*b*-butadiene-*b*-styrene) nanocomposites. *Compos Part B-Eng.* 2016;90:315-25.

- [14] Stankovich S, Dikin DA, Dommett GH, Kohlhaas KM, Zimney EJ, Stach EA, et al. Graphene-based composite materials. *Nature*. 2006;442(7100):282-6.
- [15] Geim AK. Graphene: status and prospects. *Science*. 2009;324(5934):1530-4.
- [16] Park O-K, Chae H-S, Park GY, You N-H, Lee S, Bang YH, et al. Effects of functional group of carbon nanotubes on mechanical properties of carbon fibers. *Compos Part B-Eng*. 2015;76:159-66.
- [17] Yu M-F, Lourie O, Dyer MJ, Moloni K, Kelly TF, Ruoff RS. Strength and breaking mechanism of multiwalled carbon nanotubes under tensile load. *Science*. 2000;287(5453):637-40.
- [18] Lee C, Wei X, Kysar JW, Hone J. Measurement of the elastic properties and intrinsic strength of monolayer graphene. *Science*. 2008;321(5887):385-8.
- [19] Kim P, Shi L, Majumdar A, McEuen P. Thermal transport measurements of individual multiwalled nanotubes. *Phys Rev Lett*. 2001;87(21):215502.
- [20] Ando Y, Zhao X, Shimoyama H, Sakai G, Kaneto K. Physical properties of multiwalled carbon nanotubes. *Int J of Inorg Mater*. 1999;1(1):77-82.
- [21] Balandin AA, Ghosh S, Bao W, Calizo I, Teweldebrhan D, Miao F, et al. Superior thermal conductivity of single-layer graphene. *Nano Lett*. 2008;8(3):902-7.
- [22] Du X, Skachko I, Barker A, Andrei EY. Approaching ballistic transport in suspended graphene. *Nat Nanotechnol*. 2008;3(8):491-5.
- [23] El Moumen A, Tarfaoui M, Lafdi K. Mechanical characterization of carbon nanotubes based polymer composites using indentation tests. *Compos Part B-Eng*. 2017;114:1-7.
- [24] Tarfaoui M, Lafdi K, El Moumen A. Mechanical properties of carbon nanotubes based polymer composites. *Compos Part B-Eng*. 2016;103:113-21.
- [25] Bafana AP, Yan X, Wei X, Patel M, Guo Z, Wei S, et al. Polypropylene nanocomposites reinforced with low weight percent graphene nanoplatelets. *Compos Part B-Eng*. 2017;109:101-7.
- [26] Lin F, Xiang Y, Shen H-S. Temperature dependent mechanical properties of graphene reinforced polymer nanocomposites – A molecular dynamics simulation. *Compos Part B-Eng*. 2017;111:261-9.
- [27] Novoselov KS, Falko VI, Colombo L, Gellert PR, Schwab MG, Kim K. A roadmap for graphene. *Nature*. 2012;490(7419):192-200.
- [28] Geim AK, Novoselov KS. The rise of graphene. *Nat Mater*. 2007;6(3):183-91.
- [29] Allen MJ, Tung VC, Kaner RB. Honeycomb Carbon: A Review of Graphene. *Chem Rev*. 2010;110(1):132-45.

- [30] Li C, Chou T-W. A structural mechanics approach for the analysis of carbon nanotubes. *Int J Solids Struct.* 2003;40(10):2487-99.
- [31] Cao A, Xu C, Liang J, Wu D, Wei B. X-ray diffraction characterization on the alignment degree of carbon nanotubes. *Chem Phys Lett.* 2001;344(1–2):13-7.
- [32] Ferrari AC, Robertson J. Interpretation of Raman spectra of disordered and amorphous carbon. *Phys Rev B.* 2000;61(20):14095.
- [33] Saito R, Hofmann M, Dresselhaus G, Jorio A, Dresselhaus M. Raman spectroscopy of graphene and carbon nanotubes. *Adv Phys.* 2011;60(3):413-550.
- [34] Yang S-Y, Lin W-N, Huang Y-L, Tien H-W, Wang J-Y, Ma C-CM, et al. Synergetic effects of graphene platelets and carbon nanotubes on the mechanical and thermal properties of epoxy composites. *Carbon.* 2011;49(3):793-803.
- [35] Liu W-W, Chai S-P, Mohamed AR, Hashim U. Synthesis and characterization of graphene and carbon nanotubes: A review on the past and recent developments. *J Ind Eng Chem.* 2014;20(4):1171-85.
- [36] Siddiqui NA, Li EL, Sham M-L, Tang BZ, Gao SL, Mäder E, et al. Tensile strength of glass fibres with carbon nanotube–epoxy nanocomposite coating: Effects of CNT morphology and dispersion state. *Compos Part A-Appl Sci.* 2010;41(4):539-48.
- [37] Zhou Y, Pervin F, Lewis L, Jeelani S. Experimental study on the thermal and mechanical properties of multi-walled carbon nanotube-reinforced epoxy. *Mat Sci Eng A-Struct.* 2007;452:657-64.
- [38] Bai J, Allaoui A. Effect of the length and the aggregate size of MWNTs on the improvement efficiency of the mechanical and electrical properties of nanocomposites-experimental investigation. *Compos Part A-Appl Sci.* 2003;34(8):689-94.
- [39] Agari Y, Uno T. Thermal conductivity of polymer filled with carbon materials: effect of conductive particle chains on thermal conductivity. *J Poly Sc.* 1985;30(5):2225-35.
- [40] Wang F, Drzal LT, Qin Y, Huang Z. Enhancement of fracture toughness, mechanical and thermal properties of rubber/epoxy composites by incorporation of graphene nanoplatelets. *Compos Part A-Appl Sci.* 2016;87:10-22.
- [41] Martin-Gallego M, Verdejo R, Khayet M, de Zarate JMO, Essalhi M, Lopez-Manchado MA. Thermal conductivity of carbon nanotubes and graphene in epoxy nanofluids and nanocomposites. *Nanoscale Res Lett.* 2011;6(1):1-7.
- [42] Han Z, Fina A. Thermal conductivity of carbon nanotubes and their polymer nanocomposites: a review. *Prog Polym Sci.* 2011;36(7):914-44.

- [43] Singha S, Thomas MJ. Dielectric properties of epoxy nanocomposites. *IEEE T Dielect El In.* 2008;15(1):12-23.
- [44] Poh CL, Mariatti M, Noor AFM, Sidek O, Chuah TP, Chow SC. Dielectric properties of surface treated multi-walled carbon nanotube/epoxy thin film composites. *Compos Part B-Eng.* 2016;85:50-8.

ACCEPTED MANUSCRIPT

Fig. 1. SEM images of (a) GNP and (b) MWCNT

Fig. 2. HRTEM images of GNP with magnification of (a) 7,000X and (b) 690,000X and MWCNT with magnification of (c) 97,000X and (d) 690,000X

Fig. 3. XRD patterns of (a) GNP and (b) MWCNT

Fig. 4. Raman spectrum of (a) GNP and (b) MWCNT

Fig. 5. Tensile stress–strain curves of a neat epoxy and the epoxy composites with 1%, 3%, and 5% weight percentage of GNP and MWCNT

Fig. 6. Flexural stress–strain curves of a neat epoxy and the epoxy composites with 1%, 3%, and 5% weight percentage of GNP and MWCNT

Fig. 7. SEM images of fracture surfaces of Epoxy/GNP (a) 1,000X, (b) 3,000X and (c) 5,000X

Fig. 8. SEM images of fracture surfaces of Epoxy/MWCNT (a) 10,000X, (b) 150,000X (c) 200,000X

Fig. 9. HRTEM images of Epoxy/GNP at magnification of (a) 9,000X, (b) 19,000X and Epoxy/MWCNT at magnification of (c) 71,000X and (d) 145,000X

Fig. 10. Thermal conductivity of neat epoxy and epoxy composites with 0.5%, 1% and 3% weight percentage of GNP and MWCNT

Fig. 11. Frequency dependent dielectric constant of neat epoxy and epoxy composites with 0.5%, 1% and 3% weight percentage of GNP and MWCNT

Fig. 12. Frequency dependent dielectric loss of neat epoxy and epoxy composites with 0.5%, 1% and 3% weight percentage of GNP and MWCNT.

Table 1. Descriptions of the samples.

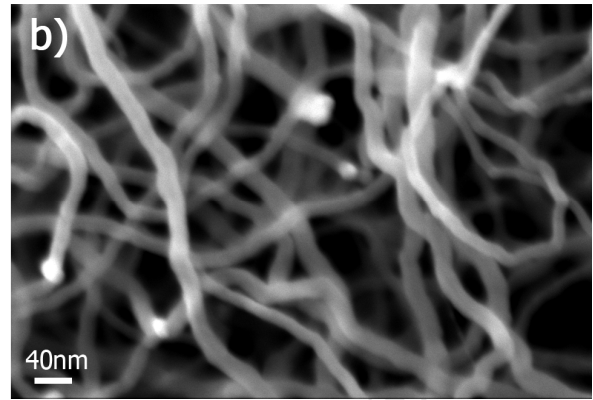
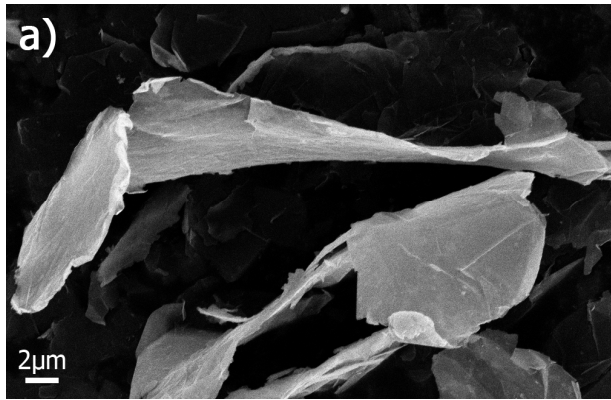
Samples	Descriptions
Epoxy/MWCNT	Epoxy filled with MWCNT
Epoxy/MWCNT 0.5	Epoxy filled with 0.5 wt% MWCNT
Epoxy/MWCNT 1	Epoxy filled with 1 wt% MWCNT
Epoxy/MWCNT 3	Epoxy filled with 3 wt% MWCNT
Epoxy/GNP	Epoxy filled with GNP
Epoxy/GNP 0.5	Epoxy filled with 0.5 wt% GNP
Epoxy/GNP 1	Epoxy filled with 1 wt% GNP
Epoxy/GNP 3	Epoxy filled with 3 wt% GNP

Table 2. Raman intensity of GNP and MWCNT.

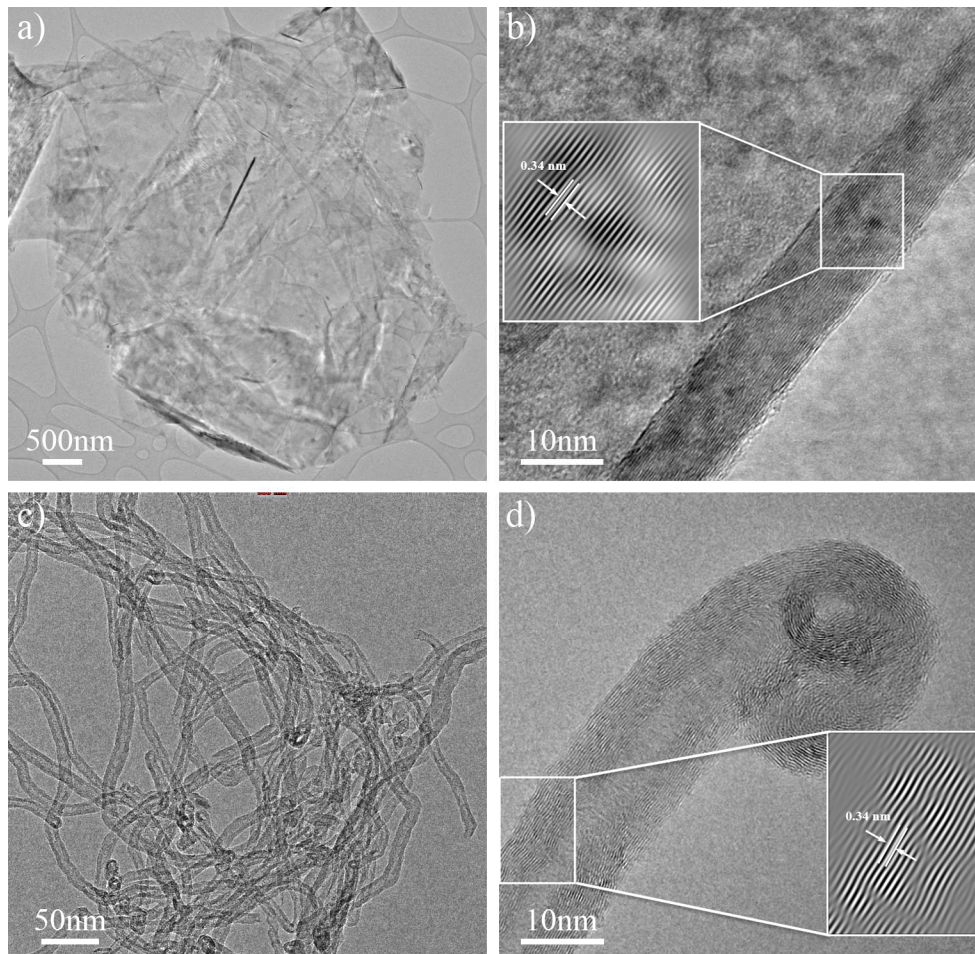
Intensity	I_D	I_{D^*}	I_G	I_D/I_G	I_{D^*}/I_G
GNP	953.13	1760.60	2647.94	0.36	0.66
MWCNT	3967.65	1428.44	2343.75	1.69	0.61

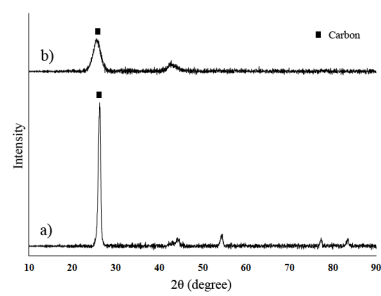
Table 3. Tensile and flexural properties of Epoxy/GNP and Epoxy/MWCNT.

Samples	Tensile Strength (MPa)	Tensile Modulus (GPa)	Tensile Fracture Strain (%)	Flexural Strength (MPa)	Flexural Modulus (GPa)	Flexural Fracture Strain (%)
Epoxy	46.46 ± 1.19	1.48 ± 0.02	4.68 ± 0.18	98.09 ± 1.62	2.42 ± 0.12	6.72 ± 0.23
Epoxy/GNP 0.5	47.48 ± 1.34	1.56 ± 0.03	4.02 ± 0.16	105.04 ± 1.86	2.76 ± 0.14	4.44 ± 0.24
Epoxy/GNP 1	51.65 ± 1.43	1.65 ± 0.04	3.61 ± 0.19	114.89 ± 2.23	3.10 ± 0.18	4.06 ± 0.26
Epoxy/GNP 3	49.78 ± 1.57	1.64 ± 0.06	3.50 ± 2.2	104.79 ± 2.47	2.89 ± 0.15	3.86 ± 0.25
Epoxy/MWCNT 0.5	50.25 ± 1.26	1.68 ± 0.02	4.13 ± 0.17	110.34 ± 1.89	2.81 ± 0.13	4.81 ± 0.24
Epoxy/MWCNT 1	58.65 ± 1.35	1.87 ± 0.02	3.88 ± 0.19	126.70 ± 2.35	3.35 ± 0.16	4.62 ± 0.28
Epoxy/MWCNT 3	54.48 ± 1.54	1.69 ± 0.03	3.81 ± 2.1	117.59 ± 1.95	3.07 ± 0.15	4.48 ± 0.27

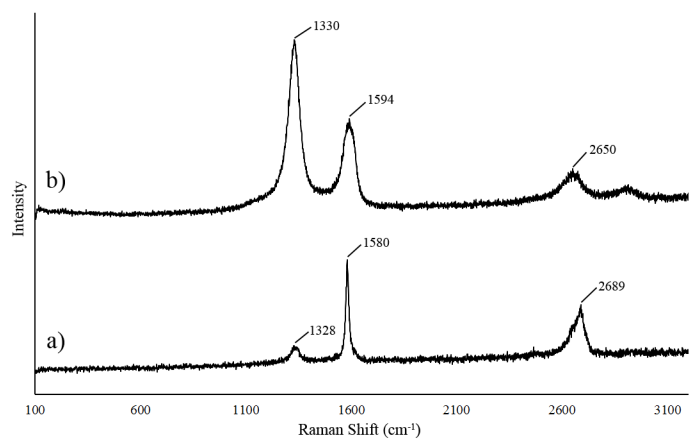


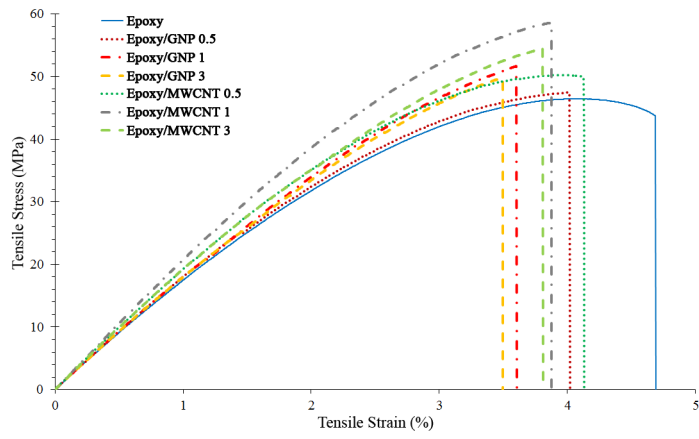
ACCEPTED MANUSCRIPT

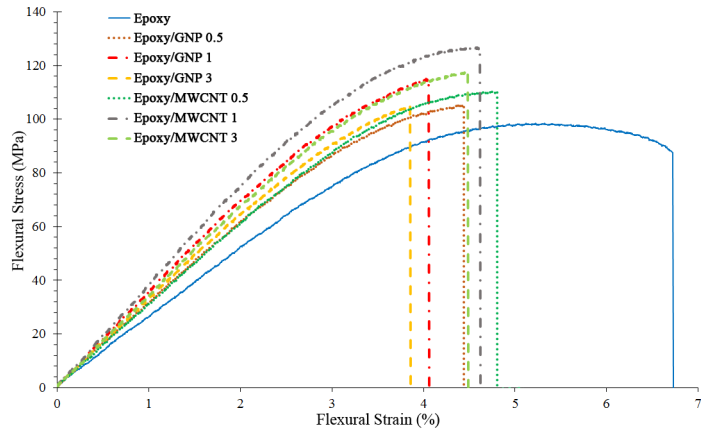


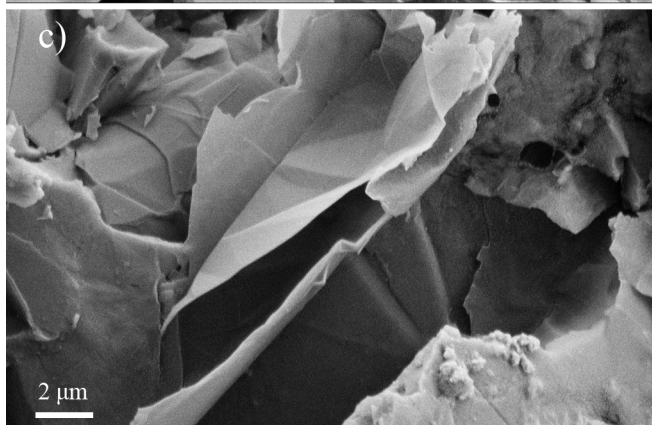
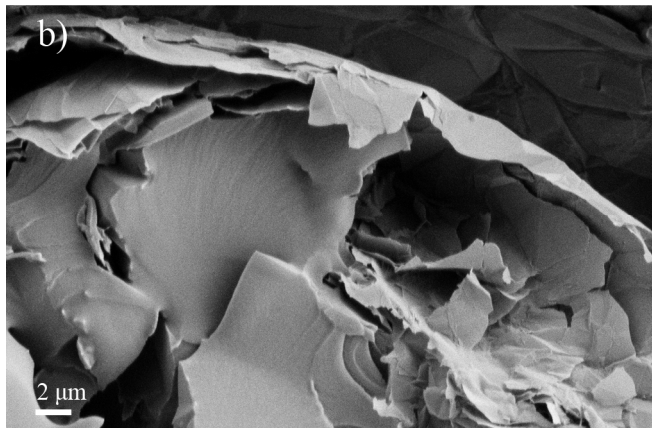
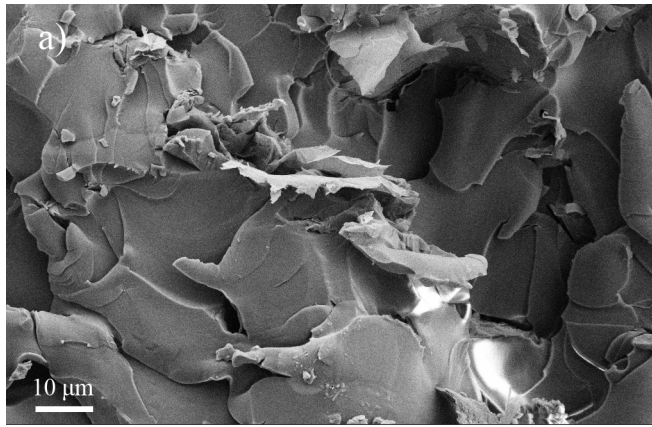


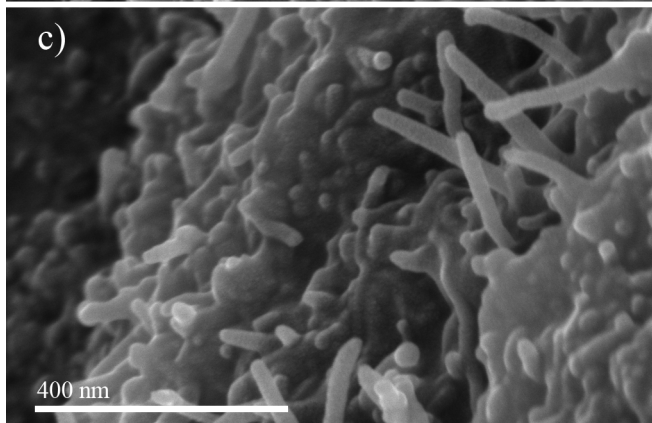
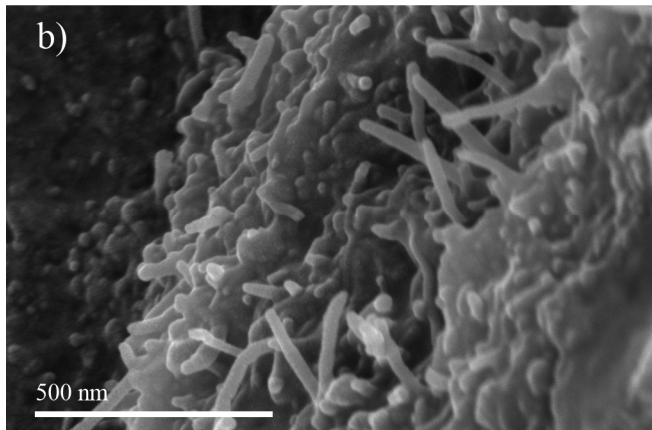
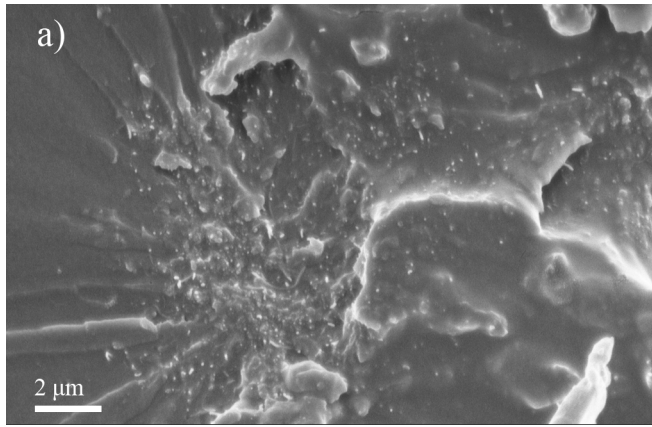
ACCEPTED MANUSCRIPT

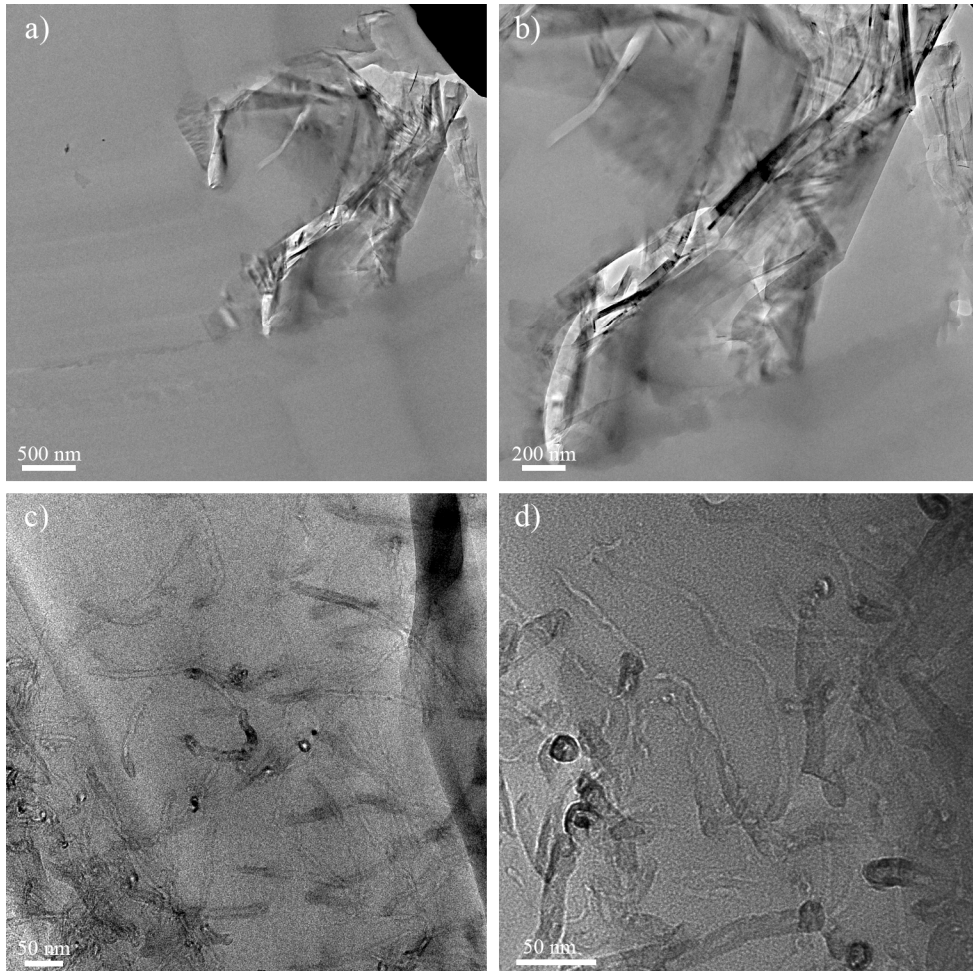


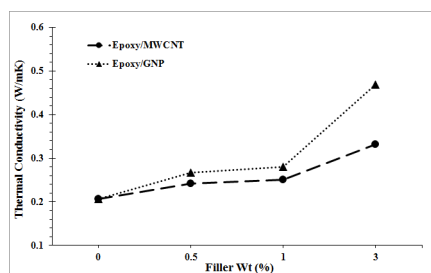












ACCEPTED MANUSCRIPT

